Journal of Physics: Conference Series **264** (2011) 012020 doi:10.1088/1742-6596/264/1/012020

Quantum simulation of relativistic quantum physics with trapped ions

C. F. Roos[1,2], R. Gerritsma[1,2], G. Kirchmair[1,2], F. Zähringer[1,2], E. Solano[3,4] and R. Blatt[1,2]

[1] Institut für Quantenoptik und Quanteninformation, Österreichische Akademie der Wissenschaften, Otto-Hittmair-Platz 1, A-6020 Innsbruck, Austria
[2] Institut für Experimentalphysik, Universität Innsbruck, Technikerstr. 25, A-6020 Innsbruck, Austria
[3] Departamento de Química Física, Universidad del País Vasco - Euskal Herriko Unibertsitatea, Apartado 644, 48080 Bilbao, Spain
[4] IKERBASQUE, Basque Foundation for Science, Alameda Urquijo 36, 48011 Bilbao, Spain

E-mail: christian.roos@uibk.ac.at

Abstract. Coupling internal and vibrational states of a string of trapped ions has proven to be an effective way of entangling the ions' internal states. This mechanism can be used for high-fidelity quantum gates, QND measurements of spin correlations and creation of large entangled states. However, spin-motion interactions are also of interest for the purpose of quantum simulations where the motional state no longer acts as an auxiliary quantum system only. Here, we describe an experiment where a laser-cooled trapped ion is set to behave as a free relativistic quantum particle.

1. Introduction

Quantum simulation aims at simulating a quantum system of interest with a controllable laboratory system described by the same mathematical model. In this way, it might be possible to simulate quantum systems that can neither be efficiently simulated on a classical computer [1] nor easily accessed experimentally. For this, the laboratory system needs to be very well understood in terms of the Hamiltonian describing it. To turn it into a useful quantum simulator, it should allow for parameter tunability and for the measurement of observables that provide important insights into the physics of the system to be simulated. There are two types of quantum simulators currently discussed in the literature. Digital quantum simulators [2, 3, 4] try to translate the unitaries describing the system dynamics into quantum circuits consisting of elementary gate operations. In this approach, a universal quantum computer could be used for efficiently simulating all quantum systems with local interactions [2]. The second class, that one might call analogue quantum simulators, builds on the principle of engineering a system having exactly the Hamiltonian one is interested in. The main motivation behind these approaches is to find solutions of problems in quantum-many body physics that cannot be efficiently simulated on classical computers. Examples include quantum phase transitions, quantum magnetism or high-temperature superconductivity.

Many proposals and experiments in this area currently focus on neutral atoms trapped in optical lattices as a possible quantum simulator [5]. The parallelism that is naturally occurring

in the interactions between atoms filling an optical lattice is a very promising starting point for simulating many-body Hamiltonians [6], and experiments demonstrating, for example, the transition from a Bose-Einstein condensate to a Mott insulator state [7] are exciting steps in this direction.

Laser-manipulated trapped ions provide another quantum optical system for which a number of proposals have been made [5, 8]. While it is more difficult to scale up ion trap systems to large numbers of particles, experiments with trapped ions offer superb possibilities for measuring observables and manipulating the system at the level of individual particles. Trapped ions have the potential of simulating quantum spin systems [9, 10, 11], spin-boson models [12] or strongly correlated phonons [13, 14]. But even systems of just a single or a few ions offer the possibility to simulate other quantum systems. The earliest example is probably the observation of C. Blockley and coworkers [15] that a resonant red-sideband interaction between two internal states of a single trapped ion and a vibrational mode is described by the Jaynes-Cummings-Hamiltonian which originally was meant to describe a two-level atom interacting with a single mode of the radiation field [16]. Other more recent examples include the suggestions to simulate quantum relativistic effects, quantum fields or particle generation [17, 18, 19, 20].

Even though the system dynamics can also be numerically simulated in experiments involving just a single ion, these experiments are nevertheless interesting as a test bed for a larger quantum simulator. For these systems, it is indeed possible to test the concept of a quantum simulator by a comparison with well-known solutions. In ref. [18], the proposal was made that a laser-manipulated trapped ion can be used to simulate the physics of a free Dirac particle. The Dirac equation for a spin-1/2 particle with rest mass m was put forward in 1928 to describe a quantum-relativistic particle. It is given by:

$$i\hbar\frac{\partial\psi}{\partial t} = (c\,\alpha\cdot\hat{\mathbf{p}} + \beta mc^2)\psi \tag{1}$$

where c is the speed of light, $\hat{\mathbf{p}}$ is the momentum operator, α and β are the Dirac matrices, and the wave functions ψ are 4-component spinors. It provides a natural description of the electron spin and predicts the existence of antimatter [21]. When extended to the case of a particle moving in a $1/r$ potential, it accurately predicts the spectrum of the hydrogen atom. However, it also predicts peculiar effects like Klein's paradox [22] and *Zitterbewegung* [23], a trembling motion of relativistic particles in the absence of an external potential. For electrons, this motion would have a very small amplitude ($\approx 10^{-13}$ m) and an extremely high frequency ($\approx 10^{21}$ Hz). It arises as an interference effect between the positive and negative energy parts of the spinor and does not appear for spinors that consist entirely of positive (or negative) energy. The real existence of *Zitterbewegung*, in relativistic quantum mechanics and in quantum field theory, has been a recurrent subject of discussion in the last years [24, 25].

Lamata *et al.* suggested [18] that the physics of a free Dirac particle could be simulated using an ion with four internal states and a set of laser beams coupling these states to the three harmonic oscillators describing the ion motion in the trapping potential. Luckily, the simulation of a free Dirac particle in one spatial dimension is much simpler. In one dimension, there is no need for introducing a four-component spinor. Instead, only a two-component spinor appears in the 1+1 version of the Dirac equation

$$i\hbar\frac{\partial\psi}{\partial t} = H_D\,\psi = (c\,\hat{p}\,\sigma_x + mc^2\,\sigma_z)\psi, \tag{2}$$

which couples only to a single motional degree of freedom. Here, σ_x and σ_z denote the usual Pauli matrices. In order to simulate the physics described by this equation with a trapped ion, the ion needs to be prepared in a desired input state and subjected to a non-relativistic quantum dynamics described by a Schrödinger Hamiltonian that has exactly the form of the

Dirac Hamiltonian H_D appearing in (2). Moreover, techniques need to be devised to in order to extract relevant physical observables such as the mean position of the particle $\langle x \rangle$ as a function of time.

2. Experimental realization

For our experiment [26], we work with a single trapped $^{40}Ca^{+}$ ion held in a linear trap with axial and transverse vibrational frequencies of about $\omega_{ax} = (2\pi)\,1.36$ MHz and $\omega_{tr} = (2\pi)\,3$ MHz, respectively. The two spinor components needed in Eq. (2) are encoded in the ion's $S_{1/2}$ ground state and the metastable $D_{5/2}$ state. A magnetic field of about 4 G is applied to lift the degeneracy of the Zeeman states. In the experiment described below, we chose to work with the states $S_{1/2}, m = 1/2$ and $D_{5/2}, m = 3/2$.

For a laser-cooled trapped ion, the first term appearing in H_D can be realized by a bichromatic laser field simultaneously coupling to the first red and blue vibrational sidebands of the ion's electronic transition of interest [27]:

$$H_{\mathrm{D}} = \hbar\eta\tilde{\Omega}(\sigma_x \cos\phi_+ - \sigma_y \sin\phi_+) \otimes ((a + a^\dagger)\cos\phi_- + i(a^\dagger - a)\sin\phi_-) \tag{3}$$

The phases $\phi_\pm$ are linear combinations of the phases ϕ_r, ϕ_b of the red- and blue-detuned light fields, $2\phi_\pm = \phi_b \pm \phi_r$, η is the Lamb Dicke parameter and $\tilde{\Omega}$ denotes the Rabi frequency. For the choice of $\phi_+ = 0$ and $\phi_- = \pi/2$, one obtains a spin-motion coupling proportional to $\sigma_x\hat{p}$. The second term of H_D could be realized by adding another light field off-resonantly coupling to an electronic transition in order to introduce a differential Stark shift described by a term proportional to σ_z. However, instead of shifting the ion's energy levels with respect to the frequency of the bichromatic light field creating the spin motion coupling, it is also possible to suitably detune the laser. By going into a reference frame where the atom-light interaction becomes time-independent, we find that the coupling is described by the Hamiltonian

$$H_D = 2\eta\Delta\tilde{\Omega}\sigma_x\hat{p} + \hbar\Omega\sigma_z, \tag{4}$$

where $\Delta = \sqrt{\hbar/(2\tilde{m}\omega_{ax})}$ is the size of the ion's ground state wave function and $\tilde{m}$ denotes the ion's mass. In this way, the Dirac Hamiltonian (2) is realized in our non-relativistic quantum system. In the ion trap system, the operators $\hat{x}$, $\hat{p}$ describing the motional state in (2) correspond to the position and the momentum of the particle in a frame rotating with the particle's oscillation frequency in the trap. By changing the strength of the off-resonant coupling term (or by changing the frequency of the bichromatic light field), the mass of the simulated particle can be varied from zero to finite values.

To determine the motional dynamics induced by the Hamiltonian (2), we need to measure the observables that characterize the ion's position as a function of time. As the motional wave packets are considerably smaller than an optical wavelength, there is no chance to determine the ion position from a simple light scattering experiment. Instead, we need to map the relevant information about the motional state onto an internal state of the ion which is then subsequently read out by a fluorescence measurement providing us with information about $\langle\sigma_z\rangle$. For this, we modify a proposal made in ref. [28] by using again a spin-motion coupling described by (3) prior to the fluorescence measurement. In this case, we make use of a state-dependent displacement operation $U_x = \exp(-ik\hat{x}\sigma_x/2)$ which is realized by applying the Hamiltonian (3) to the quantum state with $\phi_+ = \phi_- = 0$. The operation U_x followed by a measurement of σ_z is equivalent to measuring the observable

$$A(k) = U_p^\dagger\sigma_z U_p = \cos(k\hat{x})\sigma_z + \sin(k\hat{x})\sigma_y. \tag{5}$$

Here, $k = 2\eta\Omega_p t/\Delta$ is proportional to the interaction time t. If the ion's internal state is $|\uparrow\rangle$, the $+1$ eigenstate of σ_z, we have $\langle A(k)\rangle = \langle\cos(k\hat{x})\rangle$. For $|+\rangle_y$, the $+1$ eigenstate of

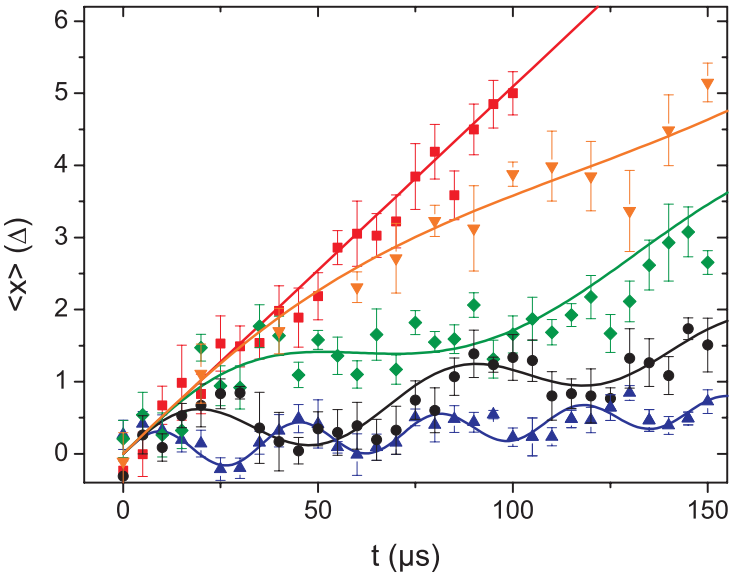

Figure 1. Expectation values $\langle\hat{x}(t)\rangle$ for particles with different masses. The linear curve (■) represents a massless particle ($\Omega = 0$) moving with the speed of light given by $c = 2\eta\tilde{\Omega}\Delta = 0.052\ \Delta/\mu$s for all curves. The other curves are for particles with increasing mass moving down from the linear curve. Their Compton wavelengths are given by $\lambda_C := 2\eta\tilde{\Omega}\Delta/\Omega = 5.4\Delta$ (▼), 2.5Δ (♦), 1.2Δ (●) and 0.6Δ (▲), respectively. The solid curves represent numerical simulations. The figure shows *Zitterbewegung* for the crossover from the relativistic $2\eta\tilde{\Omega} \gg \Omega$ to the nonrelativistic limit $2\eta\tilde{\Omega} \ll \Omega$.

σ_y, $\langle A(k)\rangle = \langle\sin(k\hat{x})\rangle$. It is also possible to measure the moments $\langle\hat{x}^k\rangle$, $k = 1, 2, \ldots$, of the distribution by taking derivatives of the expectation values of (5) with respect to k [28, 29]. For example, to measure $\langle\hat{x}\rangle$, we need to prepare $|+\rangle_y$ and calculate $\frac{d}{dk}\langle A(k)\rangle$ by applying U_x for short times (i.e., small values of k) and record the changing excitation. Moreover, a Fourier transformation of $\langle\cos(k\hat{x})\rangle$ and $\langle\sin(k\hat{x})\rangle$ yields the probability density $\langle\delta(\hat{x} - x)\rangle$ in position space.

Figure 1 demonstrates that we indeed observe *Zitterbewegung* in the motion of a relativistic particle described by the 1+1 Dirac equation. Here, we prepared the initial state $\psi(x; t = 0) = (\sqrt{2\pi}2\Delta)^{-\frac{1}{2}} e^{-\frac{x^2}{4\Delta^2}} \binom{1}{1}$ by sideband cooling and application of a $\pi/2$-pulse where $\binom{\alpha}{\beta} = \alpha|S_{1/2}, m = 1/2\rangle + \beta|D_{5/2}, m = 3/2\rangle$. The upper curve corresponds to the case of a massless particle ($\Omega = 0$) realized by making the bichromatic light field exactly resonant with the sideband transitions. Only in this case a uniform motion is observed. For a simulated particle with non-zero rest mass, obtained by tuning the centre frequency of the bichromatic laser field away from the atomic transition frequency, an oscillatory motion on top of the linear one is observed. In general, the Hamiltonian H_D entangles the spinor and motional states. For the measurement shown in Fig. 1, the spinor populations were incoherently recombined by optical pumping of the ion's $D_{5/2}$ state to $S_{1/2}, m = 1/2$ so that the ion could be prepared in an eigenstate of σ_y prior to the bichromatic laser pulse applied for measuring the particle's position. The resulting quantum states can be further characterized by reconstructing the spatial probability density $\langle\delta(\hat{x} - x)\rangle$ using again bichromatic light fields for the measurement process. Figure 2 shows another example for an input state with non-zero momentum. Here, the amplitude of the oscillatory motion vanishes after some time because positive and negative energy contributions of the state move in opposite direction and become unable to interfere after a while. The inset

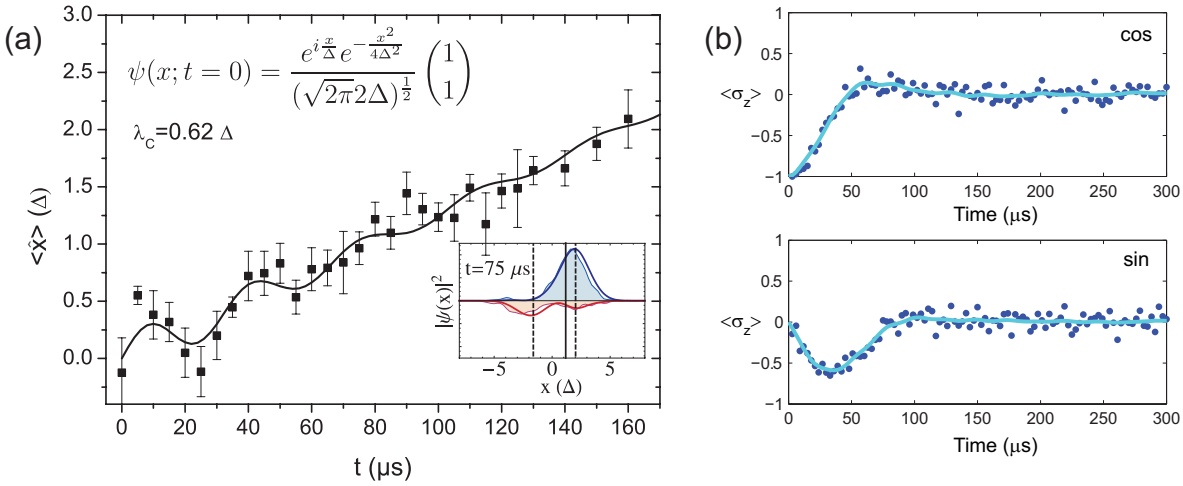

Figure 2. *Zitterbewegung* for a state with non-zero average momentum. (a) Initially, *Zitterbewegung* appears due to interference of positive and negative energy parts of the state. As these parts separate, the oscillatory motion fades away. The inset shows a position space reconstruction of the two spinor states at time $t = 75$ μs. The solid curve represents a numerical simulation. (b) Measured expectation values $\langle \cos k\hat{x} \rangle$ and $\langle \sin k\hat{x} \rangle$ used for reconstructing the probability distribution $|\psi(x)|^2$ of the spinor state plotted above the horizontal line in the inset of (a). The solid line is a fit to the data based on a convex optimization routine.

shows a reconstruction of the probability distribution based on the two spinor states after a time $t = 75$ μs. In order to reconstruct the spinor states individually, we replace the population recombination used in Fig. 1 by a projective measurement. Only if the ion scatters no light because it is projected into the state $D_{5/2}$, we use the subsequent measurement for reconstructing the probability distribution. By adding an additional π pulse to interchange the population of the spinor states, we are able to reconstruct both of them in two separate experiments. On the right-hand side of Fig. 2, the raw data $\langle \cos k\hat{x} \rangle$ and $\langle \sin k\hat{x} \rangle$ used for the reconstruction are shown. Here, $k = 2\eta\Omega_p t/\Delta$ is varied by changing the duration t of the bichromatic measurement pulse with Ω_p its Rabi frequency. To avoid unphysical negative densities, the reconstruction in position space is actually not carried out by a simple Fourier transformation. Instead, we use a convex optimization routine that realizes a least-squares fit to the data with the additional constraint of yielding non-negative densities in position space. The solid lines in Fig. 2 b are fits based on this convex optimization routine.

We consider this experiment to be an important first step that will pave the way towards more complex quantum simulations. Possible extensions include the simulation of relativistic particles in potentials that can be created by adding another ion to the setup [30]. In this extension of the work described here, the second ion interacts with another bichromatic laser field that induces a coupling proportional to $\hat{x}\sigma_x$. Now, the position operator $\hat{x}$ describes a centre-of-mass of the two-ion string. By preparing the second ion in an eigenstate of σ_x, one obtains an additional term in the Hamiltonian that looks like a linear potential for the Dirac particle encoded in the other ion. In this way, other relativistic phenomena like Klein tunneling could be observed in the setup.

Acknowledgments
We gratefully acknowledge support by the Austrian Science Fund (FWF), by the European Commission (Marie-Curie program) and by the Institut für Quanteninformation GmbH. E.S.

acknowledges support of UPV-EHU Grant GIU07/40 and EU project EuroSQIP. This material is based upon work supported in part by IARPA.

References

[1] Feynman R 1982 *Int. J. Theoret. Phys.* **21** 467–488
[2] Lloyd S 1996 *Science* **273** 1073–1078
[3] Abrams D S and Lloyd S 1997 *Phys. Rev. Lett.* **79** 2586–2589
[4] Zalka C 1998 *Proc. Roy. Soc. London A* **454** 313–322
[5] Jane E, Vidal G, Dür W, Zoller P and Cirac J I 2003 *Quantum Info. Comp.* **3** 15–37
[6] Bloch I, Dalibard J and Zwerger W 2008 *Rev. Mod. Phys.* **80** 885–964
[7] Greiner M, Mandel O, Esslinger T, Hänsch T W and Bloch I 2002 *Nature* **415** 39–44
[8] Johanning M, Varón A F and Wunderlich C 2009 *J. Phys. B* **42** 154009
[9] Porras D and Cirac J I 2004 *Phys. Rev. Lett.* **92** 207901
[10] Schmied R, Roscilde T, Murg V, Porras D and Cirac J I 2008 *New. J. Phys.* **10** 045017
[11] Friedenauer H, Schmitz H, Glueckert J, Porras D and Schaetz T 2008 *Nat. Phys.* **4** 757–761
[12] Porras D, Marquardt F, von Delft J and Cirac J I 2008 *Phys. Rev. A* **78** 010101
[13] Porras D and Cirac J I 2004 *Phys. Rev. Lett.* **93** 263602
[14] Deng X L, Porras D and Cirac J I 2008 *Phys. Rev. A* **77** 033403
[15] Blockley C A, Walls D F and Risken H 1992 *Europhys. Lett.* **17** 509–514
[16] Shore B W and Knight P L 1993 *J. Mod. Opt* **40** 1195–1238
[17] Alsing P M, Dowling J P and Milburn G J 2005 *Phys. Rev. Lett.* **94** 220401
[18] Lamata L, León J, Schätz T and Solano E 2007 *Phys. Rev. Lett.* **98** 253005
[19] Bermudez A, Martin-Delgado M A and Solano E 2007 *Phys. Rev. A* **76** 041801(R)
[20] Schützhold R, Uhlmann M, Petersen L, Schmitz H, Friedenauer A and Schätz T 2007 *Phys. Rev. Lett.* **99** 201301
[21] Anderson C D 1933 *Phys. Rev.* **43** 491–494
[22] Klein O 1929 *Z. Phys.* **53** 157–165
[23] Schrödinger E 1930 *Sitz. Preuss. Akad. Wiss. Phys.-Math. Kl.* **24** 418–428
[24] Krekora P, Su Q and Grobe R 2004 *Phys. Rev. Lett.* **93** 043004
[25] Wang Z Y and Xiong C D 2008 *Phys. Rev. A* **77** 045402
[26] Gerritsma R, Kirchmair G, Zähringer F, Solano E, Blatt R and Roos C F 2010 *Nature* **463** 68
[27] Zähringer F, Kirchmair G, Gerritsma R, Solano E, Blatt R and Roos C F 2010 *Phys. Rev. Lett.* **104** 100503
[28] Lougovski P, Walther H and Solano E 2006 *Eur. Phys. J. D* **38** 423–426
[29] Santos M F, Giedke G and Solano E 2007 *Phys. Rev. Lett.* **98** 020401
[30] Casanova J, Garcia-Ripoll J J, Gerritsma R, Roos C F and Solano E 2010 *Phys. Rev. A* **82** 020101(R)